

## An Efficient and Novel Ammonia Sensor Based on Polypyrrole/Tin Oxide/MWCNT Nanocomposite

AHMAD HUSAIN<sup>1</sup>, MOHD UROOJ SHARIQ<sup>2\*</sup> and ANEES AHMAD<sup>2</sup>

<sup>1</sup>Department of Applied Chemistry, Zakir Husain College of Engineering and Technology, Aligarh Muslim University, Aligarh-202002, India

<sup>2</sup>Department of Chemistry, Faculty of Science, Aligarh Muslim University, Aligarh-202002, India

\*Corresponding author: E-mail: [murooj17@gmail.com](mailto:murooj17@gmail.com)

Received: 23 January 2020;

Accepted: 11 March 2020;

Published online: 30 May 2020;

AJC-19904

In present study, the synthesis and characterization of a novel polypyrrole (PPy)/tin oxide (SnO<sub>2</sub>)/MWCNT nanocomposite along with pristine polypyrrole is reported. These materials have been studied for their structural and morphological properties by FT-IR spectroscopy, X-ray diffraction (XRD), scanning electron microscopy (SEM) and transmission electron microscopy (TEM) techniques. PPy/SnO<sub>2</sub>/MWCNT nanocomposite has been converted into a pellet-shaped sensor, and its ammonia sensing studies were carried out by calculating the variation in the DC electrical conductivity at different concentration of ammonia ranging from 10 to 1500 ppm. The sensing response of the sensor was determined at 1500, 1000, 500, 200, 100 and 10 ppm and found to be 70.4, 66.1, 62.2, 55.4, 50.8 and 39.7%, respectively. The sensor showed a complete reversibility at lower concentrations along with excellent selectivity and stability. Finally, a sensing mechanism was also proposed involving polarons (charge carriers) of polypyrrole and lone pairs of ammonia molecules.

**Keywords:** Polypyrrole, Tin oxide, MWCNT, Nanocomposite, Ammonia sensor.

### INTRODUCTION

Ever since it was discovered that conjugated polymers could be altered to conduct electricity through doping, an enormous amount of research has been carried out in the sphere of conducting polymers [1]. Of late, conducting polymers have gained significance in fabricating sensing devices as the chemists can tailor their chemical and physical properties according to their particular needs [2,3]. Recently conducting polymers, for instance, polyaniline, polypyrrole, polythiophene and their nanocomposites have been utilized extensively as useful materials for fabricating chemical/gas/vapour sensors [2-7]. Amid these conducting polymers, polypyrrole and its nanocomposites have engrossed notable attention owing to the ease with which they can be synthesized, reasonably superior environmental stability and surface charge properties which can easily be altered by changing the species to be doped within the materials at some point during the synthesis [7-10]. It is well established that among the various methods already employed for enhancing the chemical stability, mechanical strength and vapour-sensing properties, one is combining polypyrrole with

inorganic nanomaterials resulting in the formation of nanocomposites. Already a vast number of published reports are available for synthesizing polypyrrole/inorganic (Fe<sub>2</sub>O<sub>3</sub>, TiO<sub>2</sub>, WO<sub>3</sub>, SnO<sub>2</sub>, graphene and CNTs, *etc.*) nanocomposite based sensors by oxidative chemical polymerization for the detection of a wide array of gases and volatile organic compounds (VOCs) [7].

Owing to properties such as distinctive geometry, high reactivity and large surface area, MWCNT displays prospective applications in gas sensing devices operating at room temperatures. Literature shows that the CNTs are vulnerable to the nearby environment. The existence of NO<sub>2</sub>, O<sub>2</sub> and NH<sub>3</sub> gases and many other molecules which can either donate or accept electrons can cause the overall conductivity to alter. On account of these properties, CNTs become ideal candidates for devising nano-dimension gas-sensing materials. However, despite possessing promising properties, there are certain limitations in using CNTs such as their long recovery time, limited gas detection, weakness to humidity and other gases which limits their usage in vapour sensing and other commercial applications [11-13]. Consequently, composites of polypyrrole (PPy)

with CNTs have attracted considerable attention in the vapour sensing applications [14].

Tin(IV) oxide is an n-type semiconductor possessing a wide band-gap of 3.6 eV. Due to the presence of properties such as chemical stability, high electrical conductivity, non-stoichiometry and high transparency, it has emerged as a budding candidate for vapour sensing applications. It is a metal oxide semiconductor displaying higher sensitivity to the target gases as compared to the other available semiconductor oxides [10,13,15,16].

Ammonia gas produced as a consequence of human made and industrial activities is among the most harmful pollutants which are hazardous to both humans as well as the environment. Being extremely toxic, even its low concentrations (ppm) can cause a severe threat. When exposed in large quantities, it is accepted to cause damage to the cells of the human body, cause injuries to the skin, eyes as well as the respiratory tract (concentration >300 ppm). A vast number of gas sensing techniques are available in present times for properly controlling and detecting ammonia vapour which differs in their mechanism as well as a range of concentration respectively [7,10,17,18].

In this study, an effort was made to combine the unique properties of PPy, SnO<sub>2</sub> and MWCNT by making a novel PPy/SnO<sub>2</sub>/MWCNT nanocomposite by chemical oxidation method. The PPy/SnO<sub>2</sub>/MWCNT nanocomposite has been utilized in the fabrication of a new pellet-shaped ammonia sensor.

## EXPERIMENTAL

Pyrrole 99% (Sigma-Aldrich), ferric chloride anhydrous and methanol (Fischer Scientific, India), tin oxide nanoparticles (SnO<sub>2</sub>) and multi-walled carbon nanotubes (MWCNT) from Platonic Nanotech Pvt. Ltd., India was used in its original form. The water used for carrying out the experimentation was double distilled.

**Preparation of polypyrrole (PPy) and PPy/SnO<sub>2</sub>/MWCNT nanocomposite:** Polypyrrole (PPy) and PPy/SnO<sub>2</sub>/MWCNT nanocomposite were prepared by *in situ* oxidation polymerization method in aqueous medium using FeCl<sub>3</sub> as oxidant [8,9]. The first step in the preparation of PPy/SnO<sub>2</sub>/MWCNT nanocomposite involved the addition of 100 mg MWCNT in 100 mL of double distilled water, followed by the agitation of this mixture for 30 min. The second step was the addition of 200 mg SnO<sub>2</sub> into the above mixture and ultrasonication of the resulting mixture for an hour. After this, 2.08 mL (0.03 mol) of pyrrole was added to the suspension containing SnO<sub>2</sub> and MWCNT and this mixture was sonicated for 3 h. The preparation of ferric chloride solution was done by adding 4.86 g (0.03 mol) of it into 100 mL double distilled water. This was followed by dropwise addition of FeCl<sub>3</sub> solution into the suspension containing pyrrole, SnO<sub>2</sub> and MWCNT accompanied with continuous stirring. A black coloured slurry was obtained after 12 h, which was thoroughly washed and filtered utilizing double distilled water followed by methanol. Finally, filtered nanocomposite was dried in an air oven at 70 °C for 24 h. The pristine PPy was also prepared by a similar method in the absence of SnO<sub>2</sub> and MWCNT.

**Characterization:** The morphological, structural and chemical composition of PPy and PPy/SnO<sub>2</sub>/MWCNT nano-

composite were characterized by FTIR (Perkin-Elmer 1725 instrument), powder X-ray diffraction (XRD), field emission scanning electron microscopy and transmission electron microscopy (Bruker D8 diffractometer with CuK $\alpha$  radiation at 1.540 Å in the range of 5° ≤ 2θ ≤ 80° at 50 kV, ZEISS GEMINISem 500 and JEM 2100, JEOL Japan, respectively).

## RESULTS AND DISCUSSION

**FT-IR analysis:** The FT-IR spectra of PPy and PPy/SnO<sub>2</sub>/MWCNT nanocomposite were recorded on KBr pellets. The absorption band at 3388 cm<sup>-1</sup> in the spectra of PPy corresponds to the stretching vibration of N-H bonds [8] (Fig. 1). The characteristic absorption bands for the C=C, C=N, C-N stretching and two =C-H bending frequencies were obtained at 1550, 1310, 1192, 1088 and 1044 cm<sup>-1</sup>, respectively [8,9]. The band appeared at 920 cm<sup>-1</sup> in the spectra of PPy attributes to the C=N<sup>+</sup>-C stretching. The appearance of this band confirms the formation of polaron (charge carriers) generated as a result of doping and also suggests that PPy had been oxidized and consists of positively charged entities (N<sup>+</sup>) as shown in Fig. 1a [8,9]. For PPy/SnO<sub>2</sub>/MWCNT nanocomposite, the N-H, C=C, C=N and C-N stretching frequencies were observed at 3411.5, 1577.5, 1370.2 and 1208.6 cm<sup>-1</sup>, respectively. A slight increase in the N-H, C=C, C=N, C-N stretching was most likely caused as a result of the interaction of PPy with SnO<sub>2</sub> nanoparticles and MWCNT (Fig. 1b). In the spectrum of PPy/SnO<sub>2</sub>/MWCNT nanocomposite, a new sharp peak observed at 662.4 cm<sup>-1</sup> is due to the Sn-O-Sn stretching vibration mode and indicates the presence of SnO<sub>2</sub> nanoparticles [10]. Thus, similarities in the spectra of PPy and PPy/SnO<sub>2</sub>/MWCNT nanocomposites with the slight shifting of characteristic peaks of PPy confirmed the successful preparation of PPy/SnO<sub>2</sub>/MWCNT nanocomposite, *i.e.* entrapment of SnO<sub>2</sub> and MWCNT into the PPy matrix.

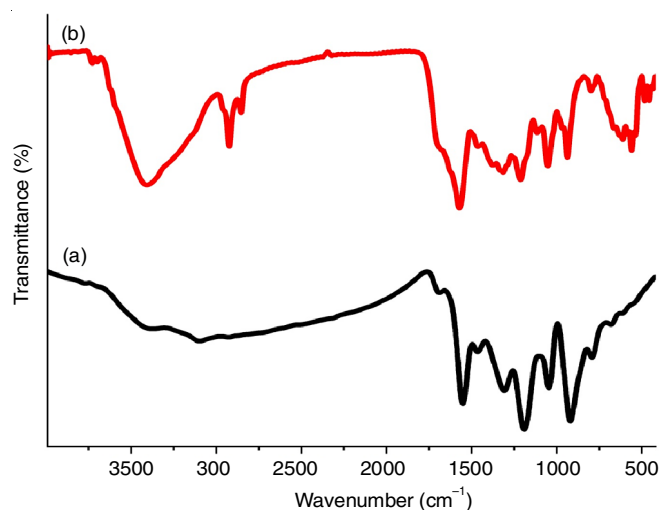


Fig. 1. FTIR spectra of (a) PPy and (b) PPy/SnO<sub>2</sub>/MWCNT nanocomposite

**X-ray diffraction (XRD) analysis:** The formation of amorphous PPy was confirmed from the appearance of a broad peak in the XRD pattern of PPy at 2θ = 24.72° as evident from Fig. 2a [8,9]. The XRD spectra of PPy/SnO<sub>2</sub>/MWCNT nanocomposite (Fig. 2b) shows that various diffraction peaks are located at 2θ angles of 26.66°, 34.08°, 38.10°, 51.96°, 54.26°, 58.10°, 60.10°, 62.10°, 64.10°, 66.10°, 68.10°, 70.10°, 72.10°, 74.10°, 76.10°, 78.10°, 80.10°, 82.10°, 84.10°, 86.10°, 88.10°, 90.10°, 92.10°, 94.10°, 96.10°, 98.10°, 100.10°, 102.10°, 104.10°, 106.10°, 108.10°, 110.10°, 112.10°, 114.10°, 116.10°, 118.10°, 120.10°, 122.10°, 124.10°, 126.10°, 128.10°, 130.10°, 132.10°, 134.10°, 136.10°, 138.10°, 140.10°, 142.10°, 144.10°, 146.10°, 148.10°, 150.10°, 152.10°, 154.10°, 156.10°, 158.10°, 160.10°, 162.10°, 164.10°, 166.10°, 168.10°, 170.10°, 172.10°, 174.10°, 176.10°, 178.10°, 180.10°, 182.10°, 184.10°, 186.10°, 188.10°, 190.10°, 192.10°, 194.10°, 196.10°, 198.10°, 200.10°, 202.10°, 204.10°, 206.10°, 208.10°, 210.10°, 212.10°, 214.10°, 216.10°, 218.10°, 220.10°, 222.10°, 224.10°, 226.10°, 228.10°, 230.10°, 232.10°, 234.10°, 236.10°, 238.10°, 240.10°, 242.10°, 244.10°, 246.10°, 248.10°, 250.10°, 252.10°, 254.10°, 256.10°, 258.10°, 260.10°, 262.10°, 264.10°, 266.10°, 268.10°, 270.10°, 272.10°, 274.10°, 276.10°, 278.10°, 280.10°, 282.10°, 284.10°, 286.10°, 288.10°, 290.10°, 292.10°, 294.10°, 296.10°, 298.10°, 300.10°, 302.10°, 304.10°, 306.10°, 308.10°, 310.10°, 312.10°, 314.10°, 316.10°, 318.10°, 320.10°, 322.10°, 324.10°, 326.10°, 328.10°, 330.10°, 332.10°, 334.10°, 336.10°, 338.10°, 340.10°, 342.10°, 344.10°, 346.10°, 348.10°, 350.10°, 352.10°, 354.10°, 356.10°, 358.10°, 360.10°, 362.10°, 364.10°, 366.10°, 368.10°, 370.10°, 372.10°, 374.10°, 376.10°, 378.10°, 380.10°, 382.10°, 384.10°, 386.10°, 388.10°, 390.10°, 392.10°, 394.10°, 396.10°, 398.10°, 400.10°, 402.10°, 404.10°, 406.10°, 408.10°, 410.10°, 412.10°, 414.10°, 416.10°, 418.10°, 420.10°, 422.10°, 424.10°, 426.10°, 428.10°, 430.10°, 432.10°, 434.10°, 436.10°, 438.10°, 440.10°, 442.10°, 444.10°, 446.10°, 448.10°, 450.10°, 452.10°, 454.10°, 456.10°, 458.10°, 460.10°, 462.10°, 464.10°, 466.10°, 468.10°, 470.10°, 472.10°, 474.10°, 476.10°, 478.10°, 480.10°, 482.10°, 484.10°, 486.10°, 488.10°, 490.10°, 492.10°, 494.10°, 496.10°, 498.10°, 500.10°.

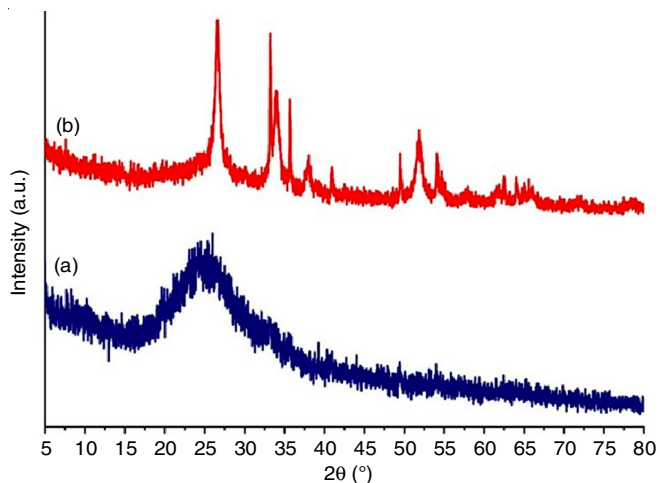


Fig. 2. XRD spectra of (a) PPy and (b) PPy/SnO<sub>2</sub>/MWCNT nanocomposite

62.38°, 65.8° confirmed the presence of SnO<sub>2</sub> nanoparticles in the as-prepared nanocomposite. These peaks correspond to the (110), (101), (200), (211), (220), (310) and (301) crystal planes of SnO<sub>2</sub>, respectively [10,19].

**SEM analysis:** The surface morphology of PPy and PPy/SnO<sub>2</sub>/MWCNT nanocomposite was studied by FE-SEM micrographs (Fig. 3). The morphology of pristine PPy (Fig. 3a) shows the agglomeration of several globular nanoparticles. In case of PPy/SnO<sub>2</sub>/MWCNT nanocomposite (Fig. 3b), the surface morphology becomes agglomeration of mostly tubular with some globular nanoparticles, which was completely different from pristine PPy. The tubular morphology was due to decoration of SnO<sub>2</sub> nanoparticle on the MWCNT on which pyrrole is polymerized. There were no free SnO<sub>2</sub> nanoparticle and MWCNT, which confirmed the polymerization of pyrrole on the surface of SnO<sub>2</sub> nanoparticle and MWCNT due to electronic interaction of PPy chains with both SnO<sub>2</sub> nanoparticle and MWCNT.

**TEM analysis:** TEM micrographs of PPy/SnO<sub>2</sub>/MWCNT nanocomposite at two different magnification *viz.* 100 nm and 50 nm are shown in Fig. 4. These micrographs revealed encapsulation of SnO<sub>2</sub> nanoparticles (dark black coloured) and MWCNT into the matrix of PPy (grey coloured part). The decoration of SnO<sub>2</sub> nanoparticles on MWCNT can be observed on which polymerization of pyrrole takes place. Thus, the formation of

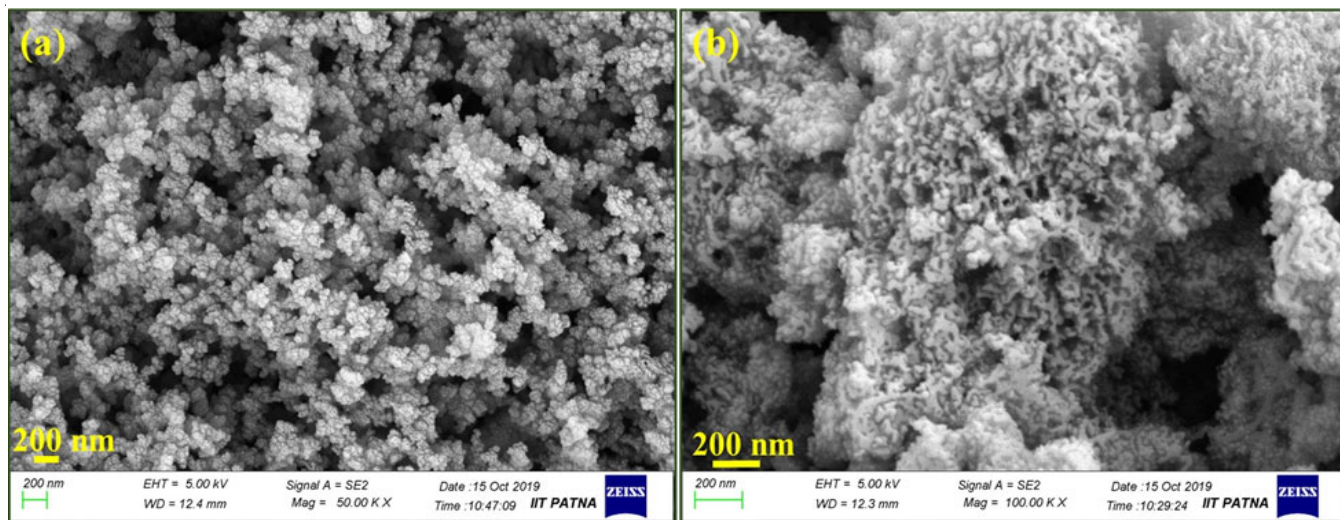


Fig. 3. FE-SEM micrographs of (a) PPy and (b) PPy/SnO<sub>2</sub>/MWCNT nanocomposite

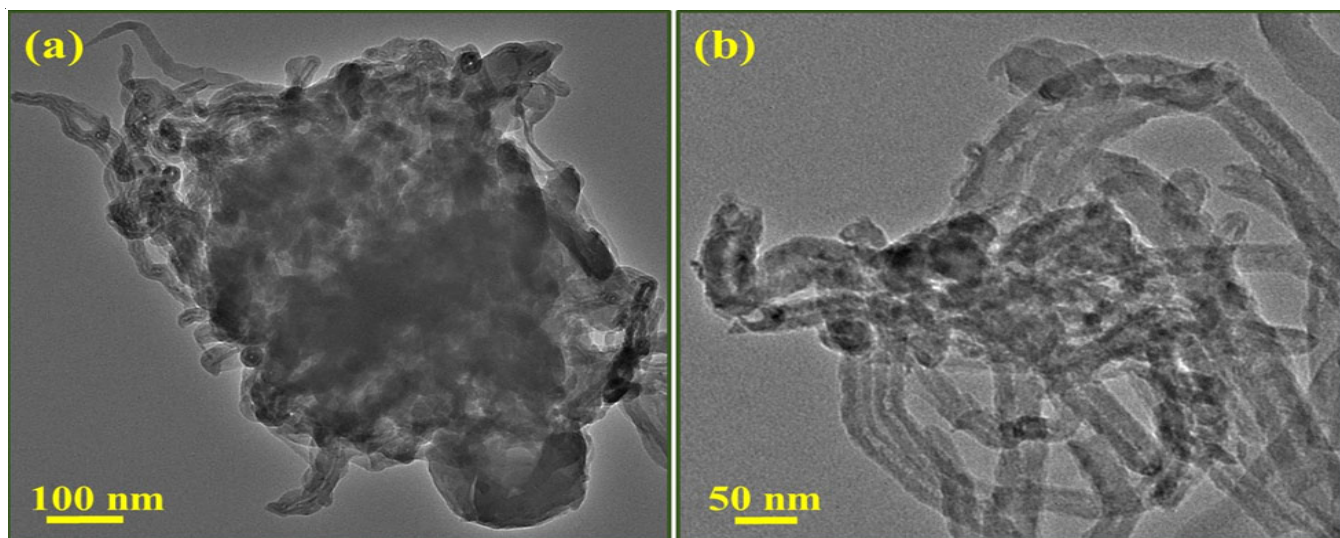


Fig. 4. TEM micrographs of PPy/SnO<sub>2</sub>/MWCNT nanocomposite at different magnifications

PPy chain on the vast surface area of SnO<sub>2</sub> nanoparticles on MWCNT provides a large number of adsorption sites which is very advantageous in the sensing.

**Sensing:** For performing the ammonia sensing experiments, 0.350 g of PPy/SnO<sub>2</sub>/MWCNT nanocomposite was converted into pellet-shaped sensing material by applying a pressure of 75 kN applied for 15 min using a hydraulic machine. A four-in-line probe with a temperature controller PID-200 (Scientific Equipment, Roorkee, India) was employed for conducting the sensing experiments of the prepared nanocomposites. All the sensing experiments were carried out at room temperature. The equation employed for the calculation of DC electrical conductivity is as follows:

$$\sigma = \frac{[\ln 2(2S/W)]}{[2\pi S(V/I)]} \quad (1)$$

where I, V, W and S represent the current (A), voltage (V), the thickness of pellet (cm) and probe spacing (cm), respectively and  $\sigma$  is the conductivity (S cm<sup>-1</sup>) [4,5].

**Sensing response:** The sensing response (%) of the prepared sensor was evaluated with respect to the change in DC electrical conductivity upon exposure to ammonia vapour for a period of 60 s. The % sensing response (S) was calculated by employing the following formula:

$$S = \frac{\Delta\sigma}{\sigma_i} \times 100 \quad (2)$$

where  $\sigma_i$  and  $\Delta\sigma$  stand for the initial DC electrical conductivity and change in the DC electrical conductivity upon exposure to ammonia for 60 s, respectively.

The first step in the sensing experiment involved attaching the sensor-pellet correctly to the four-in-line probe of device. This was followed by keeping the probe in the sealed beaker comprising of a highly evaporative solution of ammonia of known concentration for 60 s. Upon ammonia exposure, the conductivity of the sensor began to decline for the first 60 s. During this period, the sensing response was determined by calculating the variation in the conductivity. Then the sensor pellet holding probe was detached from the beaker containing ammonia solution and kept in the fresh air for 60 s. Upon exposure to air, the conductivity began to rise and reverted nearly to its initial value after 60 s (Fig. 5).

A decrease in the conductivity observed in the presence of ammonia vapour was owed to the lone pairs of electrons of

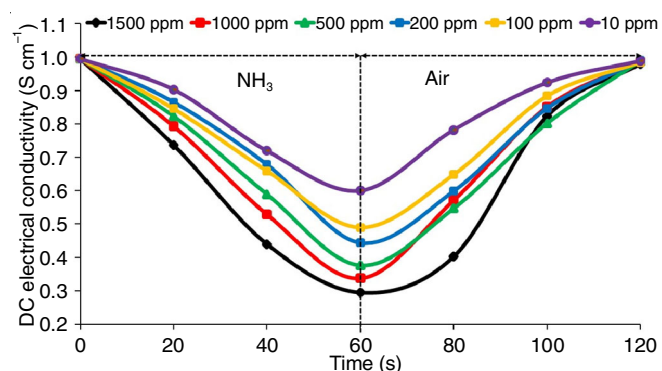


Fig. 5. Variation in DC electrical conductivity of sensor on alternate exposure of ammonia and air at different concentrations

nitrogen atoms of ammonia interacting with the charge carriers (holes) of PPy. The carriers of charge in case of conducting polymers like polypyrrole, polythiophene were polarons and bipolarons, which act similar to holes [4,5,8,9]. The factors directing their electrical conductivity is the number of these charge carriers (holes) apart from their mobility along with their extended  $\pi$ -conjugated structure. Thus alteration in the electrical conductivity of PPy could be due to any interaction which neutralizes or reduces the mobility of these charge carriers [7-9]. It is well established that ammonia being a good Lewis base readily donates its lone pair to the positively charged holes of PPy. Two possibilities arise as a result of adsorption of ammonia on the sensor surface: (a) The donation of lone pair of electrons of ammonia to the charge carriers (holes) of PPy resulting in the charge carriers getting completely neutralized and, (b) weak electronic interaction between charge carriers (holes) of PPy and the lone pair of electrons of ammonia. The possibility of a second type of interaction in this study is only because the sensor shows a dynamic response in conductivity, *i.e.* decreases in ammonia vapour and then returns to its original value upon exposure to air. This result was owed to the ammonia molecules getting desorbed from the surface of the sensor in the presence of air and thus electronic interaction between lone pairs of electrons and charge carriers of PPy disappears.

The sensing response of sensor was calculated at 1500, 1000, 500, 200, 100 and 10 ppm and found to be 70.4, 66.1, 62.2, 55.4, 50.8 and 39.7%, respectively (Fig. 6). The availability of a more substantial number of ammonia molecules (*i.e.* higher number of lone pairs) reduces the mobility of a vast amount of charge carriers leading to a greater sensing response at higher concentration. Thus, at higher concentration, a more significant change in conductivity (*i.e.* sensing response) was observed. Conversely, a minor change in conductivity is reported due to a decrease in the mobility of a smaller number of charge carriers by a comparably lesser number of ammonia molecules at lower concentrations. These results exhibited the ability of the sensor to detect ammonia vapour even at a deficient concentration of 10 ppm with a sensing response of 39.7%.

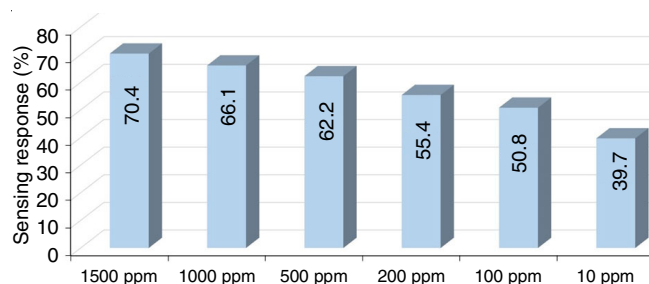


Fig. 6. Sensing response of the sensor towards ammonia at different concentrations

**Reversibility:** The sensor pellet was exposed to ammonia vapours for 30 s for studying the reversibility of the sensor. Then, sensor-pellet was removed from ammonia vapour and exposed in the air for 30 s. These procedures were repeated for three consecutive cycles comprising of a total of 180 s (Fig. 7). The sensor exhibited outstanding dynamic response, *i.e.* decrease and recovery of initial conductivity in the presence of ammonia vapour and air, respectively, confirmed that sensor was highly

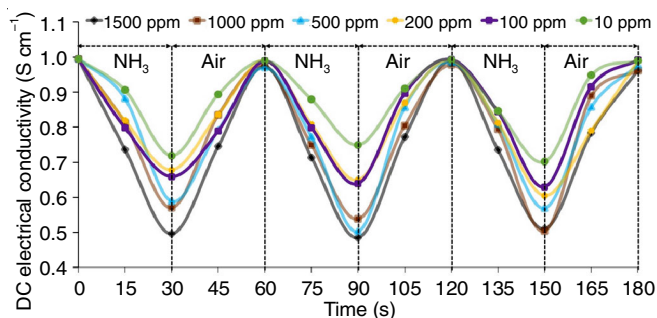


Fig. 7. Reversibility of the sensor on alternate exposure of ammonia and air at different concentrations

reversible. After three complete cycles, the conductivity returned to initial value due to desorption of ammonia molecules from the sensor surface. Thus, this ammonia sensor exhibited an excellent reversibility at lower as well as higher concentrations ranging from 1500 ppm to 10 ppm.

**Selectivity:** The fabricated sensor was evaluated for its selectivity towards ammonia vapour in the exposure of a few common volatile organic compounds (VOCs), *e.g.* ethanol, methanol, acetone and acetaldehyde at highest and the lowest concentrations, *i.e.* at 1500 ppm and 10 ppm (Fig. 8). The sensor pellet was first exposed in ammonia and then in all the tested VOCs, one by one for 60 s followed by the evaluation of the sensing response. The sensing response was found out to be 70.4, 30.4, 27.5, 10.3 and 8.2% towards ammonia, ethanol, methanol, acetone and acetaldehyde, respectively at 1500 ppm. This result showed that even at a high concentration of 1500 ppm, the sensor exhibited good selectivity. While at 10 ppm concentration, the sensor only responded to ammonia with a sensing response of 39.7%. Consequently, it was established that the sensor was exclusively selective towards ammonia vapour at 10 ppm.

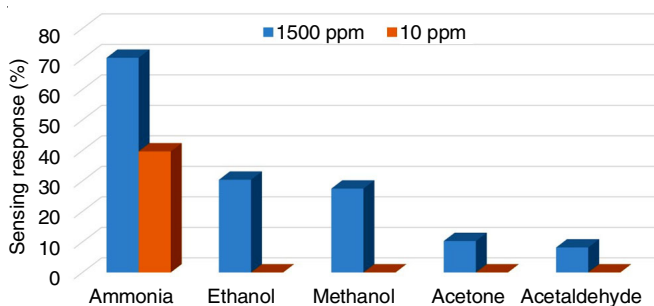


Fig. 8. Selectivity of the sensor at 1500 ppm and 10 ppm of ammonia

**Stability:** For a sensor to operate efficiently at ambient temperatures, its stability is considered to be a prerequisite. Poor stability is one of the primary concern of sensors based on conducting polymers. It is observed that their sensitivity significantly reduces after a few days [2]. Nonetheless, sensors based on nanocomposites of conducting polymers display greater stability than pristine polymers as the filler inorganic nanomaterials present in these nanocomposites exhibited exceptionally high stability [3,6,10].

In this study, the stability of sensor was determined by calculating its sensing response consecutive for 15 days at the lowest as well as highest concentrations, *i.e.* 10 ppm and 1500

ppm concentrations of ammonia (Fig. 9). At the both tested concentrations, the sensor was found to exhibit excellent stability even after 15 days.

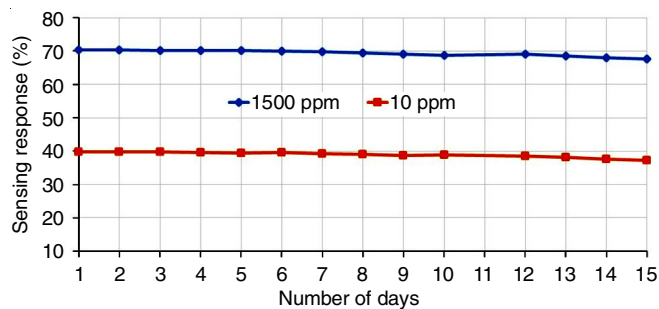


Fig. 9. Stability of the sensor at 1500 ppm and 10 ppm of ammonia

**Sensing mechanism:** The analyte gas/vapour getting adsorbed on the sensor surface is supposed to the very first step in case of conducting polymers based sensors. After adsorption, analyte molecules interact with the charge carriers (polarons/bipolarons) of the polymer affecting alteration in the electrical properties (resistance/conductivity) [2]. However, this phenomenon is more robust in the sensors based on nanocomposites of conducting polymer. These type of sensors exhibit reversibility as a result of desorption of analyte molecules from sensor surface upon exposure to air [4,5,8,9].

The basis of the sensing mechanism in this study is the adsorption/desorption phenomena of ammonia molecules on the vast surface area of sensor-pellet (Fig. 10). Ammonia, an electron-rich molecule containing lone pairs behaves as a strong Lewis base. The reduction in the mobility and charge intensity of charge carriers was caused by the interaction of lone pairs of electrons of adsorbed ammonia molecules with the electron deficient charge carriers (holes) of PPy. Consequently, an immediate decrease in conductivity was observed when sensor-pellet got exposed in the atmosphere of ammonia vapour. As soon as the sensor-pellet was exposed in air, desorption of ammonia molecules began causing a rise in the conductivity. After the ammonia molecules were completely desorbed from the sensor, the charge intensity as well as the mobility of charge carriers, recovered leading to the retrieval of initial DC electrical conductivity of the sensor.

## Conclusion

In this study, *in situ* oxidative polymerization technique was utilized for the synthesis of a novel PPy/SnO<sub>2</sub>/MWCNT nanocomposite in aqueous medium using FeCl<sub>3</sub> as an oxidant. Structural and morphological characterizations have been carried out by FT-IR spectroscopy, X-ray diffraction (XRD), scanning electron microscopy (SEM) and transmission electron microscopy (TEM). The PPy/SnO<sub>2</sub>/MWCNT nanocomposite has been used to fabricate a pellet-shaped ammonia vapour sensor operating at room temperature. The sensing response of the sensor was found to be 70.4, 66.1, 62.2, 55.4, 50.8 and 39.7 at 1500, 1000, 500, 200, 100 and 10 ppm of ammonia, respectively. The sensor also showed an excellent reversibility along with good stability. The sensor was found to be highly selective for ammonia at 1500 ppm and exclusively selective at 10 ppm. Thus, PPy/SnO<sub>2</sub>/MWCNT nanocomposite can be

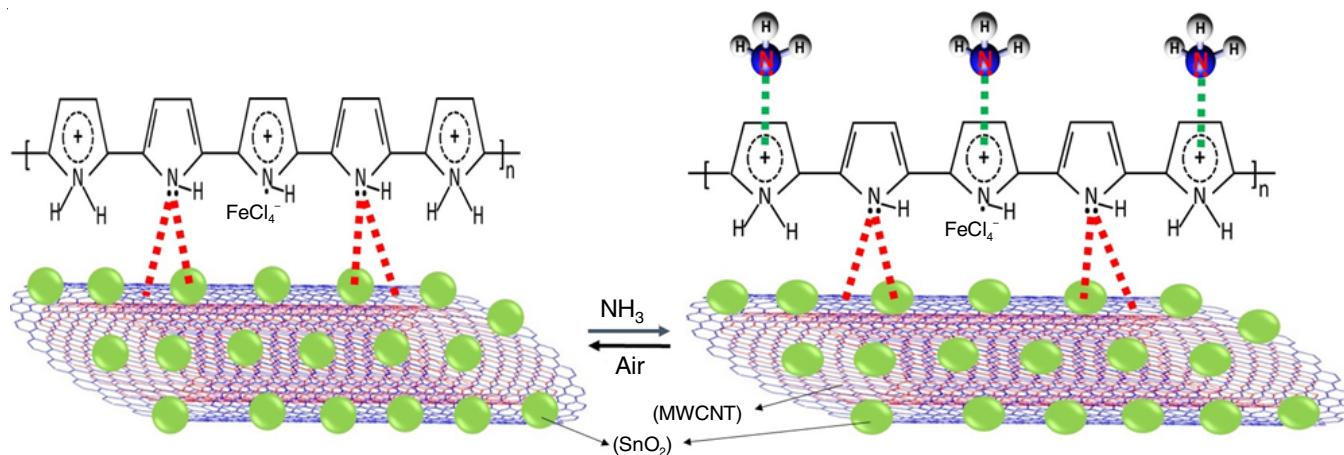


Fig. 10. Proposed sensing mechanism concerning the electronic interaction of charge carriers of PPy with lone pairs of ammonia molecules

a promising material for fabricating highly efficient ammonia sensor at room temperature.

#### ACKNOWLEDGEMENTS

The authors acknowledge to Noohul Alam (Research Scholar, IIT Patna, India) for helpful discussions.

#### CONFLICT OF INTEREST

The authors declare that there is no conflict of interests regarding the publication of this article.

#### REFERENCES

- H. Shirakawa, E.J. Louis, A.G. MacDiarmid, C.K. Chiang and A.J. Heeger, *J. Chem. Soc. Chem. Commun.*, **578**, (1977); <https://doi.org/10.1039/C39770000578>
- H. Bai and G. Shi, *Sensors*, **7**, 267 (2007); <https://doi.org/10.3390/s7030267>
- Rajesh, T. Ahuja and D. Kumar, *Sens. Actuators B Chem.*, **136**, 275 (2009); <https://doi.org/10.1016/j.snb.2008.09.014>
- A. Husain, S. Ahmad and F. Mohammad, *Mater. Today Commun.*, **20**, 100574 (2019); <https://doi.org/10.1016/j.mtcomm.2019.100574>
- A. Husain, S. Ahmad and F. Mohammad, *Mater. Chem. Phys.*, **239**, 122324 (2020); <https://doi.org/10.1016/j.matchemphys.2019.122324>
- S. Pandey, *J. Sci. Adv. Mater. Devices*, **1**, 431 (2016); <https://doi.org/10.1016/j.jsamd.2016.10.005>
- M. Šetka, J. Drbohlavová and J. Hubálek, *Sensors*, **17**, 562 (2017); <https://doi.org/10.3390/s17030562>
- A. Sultan, S. Ahmad and F. Mohammad, *RSC Adv.*, **6**, 84200 (2016); <https://doi.org/10.1039/C6RA12613H>
- A. Sultan, S. Ahmad and F. Mohammad, *Polym. Polymer Compos.*, **25**, 695 (2017); <https://doi.org/10.1177/096739111702500908>
- A. Beniwal and Sunny, *Sens. Actuators B Chem.*, **296**, 126660 (2019); <https://doi.org/10.1016/j.snb.2019.126660>
- K.S. Ibrahim, *Carbon Lett.*, **14**, 131 (2013); <https://doi.org/10.5714/CL.2013.14.3.131>
- S. Kumar, V. Pavelyev, P. Mishra and N. Tripathi, *Sens. Actuators A Phys.*, **283**, 174 (2018); <https://doi.org/10.1016/j.sna.2018.09.061>
- N. Van Hieu, L.T.B. Thuy and N.D. Chien, *Sens. Actuators B Chem.*, **129**, 888 (2008); <https://doi.org/10.1016/j.snb.2007.09.088>
- N. Van Hieu, N.Q. Dung, P.D. Tam, T. Trung and N.D. Chien, *Sens. Actuators B Chem.*, **140**, 500 (2009); <https://doi.org/10.1016/j.snb.2009.04.061>
- S. Das and V. Jayaraman, *Prog. Mater. Sci.*, **66**, 112 (2014); <https://doi.org/10.1016/j.pmatsci.2014.06.003>
- G. Velmathi, S. Mohan and R. Henry, *IETE Tech. Rev.*, **33**, 323 (2016); <https://doi.org/10.1080/02564602.2015.1080603>
- B. Timmer, W. Olthuis and A. Berg, *Sens. Actuators B Chem.*, **107**, 666 (2005); <https://doi.org/10.1016/j.snb.2004.11.054>
- D. Kwak, Y. Lei and R. Maric, *Talanta*, **204**, 713 (2019); <https://doi.org/10.1016/j.talanta.2019.06.034>
- W. Chen, Q. Zhou, F. Wan and T. Gao, *J. Nanomater.*, **2012**, 612420 (2012); <https://doi.org/10.1155/2012/612420>